



Observation of the open-charm tetraquark state $T_{cs0}^*(2870)^0$ in the $B^- \rightarrow D^- D^0 K_S^0$ decay

LHCb collaboration[†]

Abstract

An amplitude analysis of $B^- \rightarrow D^- D^0 K_S^0$ decays is performed using proton-proton collision data, corresponding to an integrated luminosity of 9 fb^{-1} , collected with the LHCb detector at center-of-mass energies of 7, 8, and 13 TeV. A resonant structure of spin-parity 0^+ is observed in the $D^0 K_S^0$ invariant-mass spectrum with a significance of 5.3σ . The mass and width of the state, modeled with a Breit–Wigner lineshape, are determined to be $2883 \pm 11 \pm 6 \text{ MeV}/c^2$ and $87_{-47}^{+22} \pm 6 \text{ MeV}$ respectively, where the first uncertainties are statistical and the second systematic. These properties and the quark content are consistent with those of the open-charm tetraquark state $T_{cs0}^*(2870)^0$ observed previously in the $D^+ K^-$ final state of the $B^- \rightarrow D^- D^+ K^-$ decay. This result confirms the existence of the $T_{cs0}^*(2870)^0$ state in a new decay mode. The $T_{cs1}^*(2900)^0$ state, reported in the $B^- \rightarrow D^- D^+ K^-$ decay, is also searched for in the $D^0 K_S^0$ invariant-mass spectrum of the $B^- \rightarrow D^- D^0 K_S^0$ decay, without finding evidence for it.

Submitted to Phys. Rev. Lett.

© 2024 CERN for the benefit of the LHCb collaboration. [CC BY 4.0 licence](#).

[†]Authors are listed at the end of this paper.

Hadrons composed of more than three quarks, referred to in this Letter as exotic states, play a unique role in understanding the confinement mechanism of the strong interaction [1, 2]. In two decades of advances after the $\chi_{c1}(3872)$ discovery in 2003 [3], a variety of exotic states has been experimentally observed. These include the charmonium-like tetraquark $T_{cc1}(3900)^+$ [4, 5], tetraquarks with two or four charm quarks $T_{cc}(3875)^+$ [6, 7] and $T_{cc\bar{c}\bar{c}}(6900)^0$ [8–10], respectively, and pentaquark P_{cc}^+ and P_{ccs}^0 states [11–15]. In 2020, two states $T_{cs0}^*(2870)^0$ and $T_{cs1}^*(2900)^0$, with spin-parity $J^P = 0^+$ and 1^- respectively, and minimum quark content $cs\bar{u}\bar{d}$, were observed by the LHCb collaboration in the D^+K^- final state of the $B^- \rightarrow D^-D^+K^-$ decay [16, 17]. This was the first observation of manifestly exotic hadrons with a single charm quark, opening a new avenue for understanding the quark-binding mechanism. The existence of these states was confirmed in the D^+K^- invariant-mass spectrum of the $B^- \rightarrow D^{*-}D^+K^-$ decay [18]. Charged open-charm tetraquarks were searched for in $B^0 \rightarrow D^+D^-K_S^0$ decays, but without any significant signal [19]. Recently, two new open-charm tetraquarks $T_{cs0}^*(2900)^{0/++}$, with $J^P = 0^+$ and minimum quark content $c\bar{s}\bar{u}\bar{d}/c\bar{s}u\bar{d}$, were observed in the $D_s^+\pi^\mp$ final state of the $B^0 \rightarrow \bar{D}^0D_s^+\pi^-$ and $B^+ \rightarrow D^-D_s^+\pi^+$ decays [20, 21]. Charge conjugation of states and decays is implied throughout this Letter.

Studies have been carried out to understand the nature and internal structure of the $T_{cs0}^*(2870)^0$ and $T_{cs1}^*(2900)^0$ states, collectively referred to as T_{cs}^{*0} states hereafter. They can be interpreted as compact tetraquarks [22–29] or $D^{(*)}\bar{K}^*$ hadronic molecules [30–37]. In either case, assuming isospin symmetry is respected, the T_{cs}^{*0} states should decay to both D^+K^- and $D^0\bar{K}^0$ final states with similar rates [37, 38], as the two systems have the same minimum quark content. The two T_{cs}^{*0} structures can also be explained as kinematically generated singularities, originating from intermediate three-hadron loop diagrams [38]. In this scenario, the T_{cs}^{*0} structures produced in the $B^- \rightarrow D^-T_{cs}^{*0}$ decay exhibit larger decay rates into the D^+K^- final state than into the $D^0\bar{K}^0$ final state [38]. Given the present limited experimental inputs, it is still difficult to establish which interpretation is more likely [39].

This Letter presents an amplitude analysis of the $B^- \rightarrow D^-D^0\bar{K}^0$ decay, where the T_{cs}^{*0} resonances could be observed in the $D^0\bar{K}^0$ final state, and the \bar{K}^0 meson is reconstructed in the K_S^0 mass eigenstate. The analysis is performed using proton-proton (pp) collision data collected by the LHCb experiment, corresponding to an integrated luminosity of 9 fb^{-1} at center-of-mass energies of 7, 8 and 13 TeV. The LHCb detector [40, 41] is a single-arm forward spectrometer covering the pseudorapidity range $2 < \eta < 5$. The detector elements that are particularly relevant to this analysis includes a silicon-strip vertex detector surrounding the pp interaction region that allows c and b hadrons to be identified from their characteristically long flight distance, a high-precision tracking system to measure the momentum, p , of charged particles, and two ring-imaging Cherenkov detectors to perform particle identification (PID) for charged hadrons. The online event selection of $B^- \rightarrow D^-D^0K_S^0$ decays is performed using a trigger, which consists of a hardware stage based on information from the calorimeter and muon systems, followed by a software stage, which applies a full event reconstruction.

In the offline analysis, B^- candidates are selected by combining D^- , D^0 and K_S^0 candidates. The D^- and K_S^0 mesons are reconstructed in $D^- \rightarrow K^+\pi^-\pi^-$ and $K_S^0 \rightarrow \pi^+\pi^-$ decays, respectively, while the D^0 meson is formed according to either the $D^0 \rightarrow K^-\pi^+$ or the $D^0 \rightarrow K^-\pi^+\pi^-\pi^+$ decay. The final-state tracks are required to be positively identified as pions or kaons by the PID detectors, to have a large transverse momentum (p_T) and

to be well separated from any pp collision vertex (PV). The D^- , D^0 and K_S^0 candidates should have reconstructed decay vertices of good fit quality and invariant masses consistent with known values from Ref. [42]. The reconstructed decay vertex of the B^- meson is required to have a good fit quality and be significantly displaced from its associated PV, defined as the PV which aligns best with the flight direction of the B^- candidate. To improve the experimental resolution on the reconstructed B^- invariant mass, $m_{D^-D^0K_S^0}$, a kinematic fit to the whole decay chain is performed, with the D^- , D^0 and K_S^0 invariant masses constrained to their known values [42] and the B^- momentum constrained to point back to its associated PV [43]. The background, dominated by random combinations of D^- , D^0 and K_S^0 candidates, is further suppressed by a boosted decision tree (BDT) [44,45] implemented in the TMVA toolkit [46]. The BDT classifier is trained using a sample of simulated $B^- \rightarrow D^-D^0K_S^0$ candidates as signal sample, and candidates with B^- mass exceeding $5500 \text{ MeV}/c^2$ from data as background sample. Training variables include those characterizing the decay topology, particle transverse momenta, vertex fit quality and particle identification information for pions and kaons. The requirement on the BDT classifier maximizes the figure of merit $N_S^2/(N_S + N_B)^{3/2}$ [16], where N_S and N_B represent the signal and background yields in the signal region, which is defined as $\pm 20 \text{ MeV}/c^2$ around the known B^- mass [42]. Possible physics backgrounds are investigated, notably the $B \rightarrow D^*D^-K_S^0$ decay with $D^* \rightarrow D^0\pi/\gamma$, where the π/γ particle is not reconstructed, and the $B^- \rightarrow D^0K_S^0K^+\pi^-\pi^-$ five-body decay. The former is shifted and well separated from the B^- signal, and the latter is suppressed to a negligible level by requiring that the vertices of the D^- and B^- candidates are well separated.

A simulated sample of $B^- \rightarrow D^-D^0K_S^0$ decays, generated with the software packages described in Refs. [47–50], is used to model the effects of the detector acceptance and the imposed selection requirements. The B^- transverse momentum and rapidity distribution, as well as the PID and trigger responses are weighted to match the data. The simulated decays are subjected to the same reconstruction and selection procedures as the data.

In order to extract the yield of the signal decay mode, an unbinned extended maximum-likelihood fit is performed to the $m_{D^-D^0K_S^0}$ distribution. The signal is described by a combination of two Gaussian functions with a shared mean value. The combinatorial background is modeled by an exponential function. The relative proportions of the two Gaussian functions and the ratio of their widths are fixed to values obtained in the simulated samples, while the remaining parameters are floated in the fit. The $m_{D^-D^0K_S^0}$ distribution is shown in Fig. 1(a), together with the fit results. In the signal region, the yield and fraction of the $B^- \rightarrow D^-D^0K_S^0$ signal decay are determined to be 1540 ± 40 and $f_s = (92.6 \pm 0.6)\%$, respectively.

The Dalitz plot of the $B^- \rightarrow D^-D^0K_S^0$ decay, represented by the squared two-body invariant masses $m_{D^-K_S^0}^2$ and $m_{D^0K_S^0}^2$, is shown in Fig. 1(b) for candidates in the B^- signal region. The Dalitz-plot variables are calculated with the masses of B^- , D^- , D^0 and K_S^0 mesons constrained to their known values [42] and the B^- momentum constrained to point back to its associated PV [43]. Excited D_s^- mesons, D_{sJ}^{*-} , are clearly visible in the low $m_{D^-K_S^0}^2$ region. An amplitude analysis is performed to investigate all resonance structures in the $B^- \rightarrow D^-D^0K_S^0$ decays. The total probability density function (PDF) is described as the sum of those for the B^- signal, \mathcal{P}_s , and the combinatorial background, \mathcal{P}_b , with the signal fraction f_s fixed to the value measured by the fit to the $m_{D^-D^0K_S^0}$ mass spectrum. The PDF of the combinatorial background is determined using data in the mass region

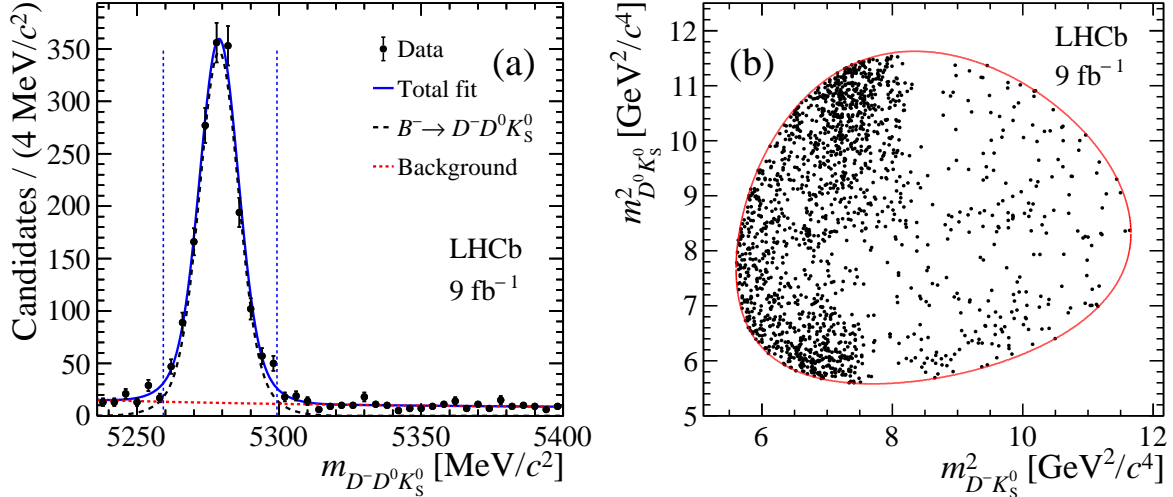


Figure 1: (a) Invariant-mass distribution of the B^- candidates with the fit results also shown. The blue dashed lines illustrate the B^- signal region corresponding to a signal yield of 1540 ± 40 with a purity of $(92.6 \pm 0.6)\%$. (b) Dalitz plot of B^- candidates within the signal region. The red solid curve represents the kinematic boundary.

$5350 < m_{D^-D^0K_S^0} < 5565$ MeV/c². For the signal PDF, contributions from two interfering decay sequences are considered: $B^- \rightarrow D_{sJ}^{*-}(\rightarrow D^-K_S^0)D^0$ and $B^- \rightarrow T_{cs}^{*0}(\rightarrow D^0K_S^0)D^-$, collectively denoted as $B^- \rightarrow R(\rightarrow ab)c$. For each decay sequence, various D_{sJ}^{*-} or T_{cs}^{*0} components are investigated, and each component contributes to the decay with an independent amplitude, $\mathcal{M}_R(m_{ab}, \theta_{ab}|\vec{\omega})$, where θ_{ab} is the angle between the momenta of a and the B^- in the R rest frame, and the m_{ab} variable is the invariant mass of the ab system [21]. The set of free parameters $\vec{\omega}$ includes the complex coupling for each amplitude, and the masses and widths of unknown states. The distribution of candidates in the Dalitz plane is proportional to the squared total amplitude defined as the coherent sum of each amplitude determined by the helicity formalism [51]. Accounting for the nonuniform experimental efficiency across the Dalitz plot, $\epsilon(m_{ab}, \theta_{ab})$, the signal PDF is determined to be

$$\mathcal{P}_s(m_{ab}, \theta_{ab}|\vec{\omega}) = \frac{\epsilon(m_{ab}, \theta_{ab})}{I(\vec{\omega})} \left| \sum_R \mathcal{M}_R(m_{ab}, \theta_{ab}|\vec{\omega}) \right|^2,$$

where $I(\vec{\omega})$ is a normalization factor, and the index R runs over the considered contributions. The efficiency is determined in bins of the Dalitz plot using simulated $B^- \rightarrow D^-D^0K_S^0$ decays. The log-likelihood is

$$\ln \mathcal{L} = \sum_j \ln [f_s \mathcal{P}_s(m_{ab}^j, \theta_{ab}^j|\vec{\omega}) + (1 - f_s) \mathcal{P}_b(m_{ab}^j, \theta_{ab}^j)],$$

where the j index runs over the number of the B^- candidates in the signal region. Maximization of $\ln \mathcal{L}$ returns the estimated values of the unknown parameters.

The first model, used to fit the data, considers only resonant D_{sJ}^{*-} mesons and non-resonant (NR) components in the $D^-K_S^0$ channel. Resonances decaying strongly to two pseudoscalar mesons can only have spin-parity J^P in the natural spin-parity series: 0^+ ,

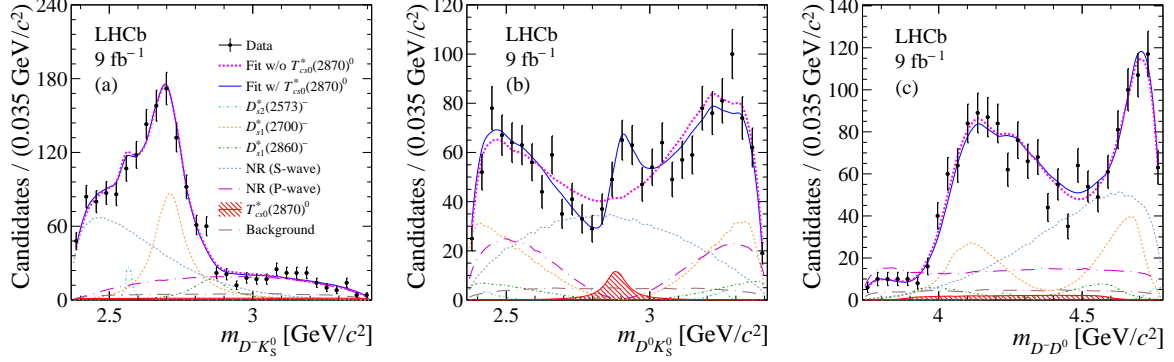


Figure 2: Mass distributions of (a) $m_{D^- K_S^0}$, (b) $m_{D^0 K_S^0}$ and (c) $m_{D^- D^0}$, together with the fit projections with (thick blue) or without (dashed magenta) the $T_{cs0}^*(2870)^0$ state. The subcomponents correspond to the fit including the $T_{cs0}^*(2870)^0$ structure.

1^- , 2^+ , *etc.* Those with masses above the $D^- K_S^0$ mass threshold, $D_{s2}^*(2573)^-$, $D_{s1}^*(2700)^-$ and $D_{s1}^*(2860)^-$, are included in the fit. The invariant-mass distribution for each state is modeled using a relativistic Breit–Wigner (RBW) function, where the Blatt–Weisskopf radius is set to 4 (GeV/c)^{-1} [52], and the masses and widths are fixed to their known values [42]. States with higher spin are less likely to be produced, and the effects of their possible presence are considered as a source of systematic uncertainty. Besides D_{sJ}^* resonances, S-wave and P-wave NR contributions are needed to model the $m_{D^- K_S^0}$ distribution, and described by an exponential and a uniform distribution, respectively. The two-body invariant-mass distributions and projections of the amplitude fit are shown in Fig. 2. With these contributions from $D^- K_S^0$ components, the $m_{D^- K_S^0}$ and $m_{D^- D^0}$ distributions are well described. However, the $m_{D^0 K_S^0}$ distribution is not well modeled, in particular around 2.9 GeV/c^2 . Alternative fits varying the D_{sJ}^* model are performed, including varying masses and widths of D_{sJ}^* resonances within their uncertainties, changing the Blatt–Weisskopf radii, using the K-matrix parameterization [53] to describe the spin-1 $D^- K_S^0$ contributions, or adding higher spin $D^- K_S^0$ resonances (*e.g.* $D_{s3}^*(2860)^-$). None of the approaches significantly improves the fit quality around $m_{D^0 K_S^0} = 2.9 \text{ GeV/c}^2$. Charmonium-like tetraquarks, $T_{c\bar{c}}^-$, decaying into the $D^- D^0$ final state are also considered in the fit, but no significant signal is found.

The amplitude fit quality is improved by including a resonant contribution in the $D^0 K_S^0$ final state, with the invariant-mass distribution modeled by a RBW distribution with floated mass and width. Various J^P assignments are tested, with the $J^P = 0^+$ giving the largest increase of the likelihood, with $2\Delta \ln \mathcal{L} = 50.7$. This additional state is denoted as T_{cs0}^{*0} in the following. The mass and width of the T_{cs0}^{*0} state are determined to be $2883 \pm 11 \text{ MeV/c}^2$ and $87_{-47}^{+22} \text{ MeV}$ respectively, and the fit fraction (FF) of the $B^- \rightarrow T_{cs0}^{*0}(\rightarrow D^0 K_S^0) D^-$ component in the total $B^- \rightarrow D^- D^0 K_S^0$ decay is $(2.6 \pm 1.2)\%$, where all uncertainties are statistical. The FF is calculated as the ratio between the phase-space integral of the squared amplitude for a single resonance to that of the total squared amplitude. The detailed results of the fit parameters are summarized in Table 3 in the End Matter. As shown in Fig. 2, for this configuration of the fit, all three invariant-mass distributions are well modeled by the fit. This fit is considered as the nominal model of the analysis. The significance of the T_{cs0}^{*0} state is evaluated with a likelihood-ratio test using

Table 1: Summary of systematic uncertainties on the mass, width and fit fraction of the T_{cs0}^{*0} state observed in the $B^- \rightarrow D^- D^0 K_S^0$ decay.

Source	Mass [MeV/ c^2]	Width [MeV]	FF [%]
f_s	0.9	1.7	0.06
Background PDF	0.6	2.1	0.09
Efficiency	0.6	3.2	0.11
Blatt–Weisskopf radii	1.2	0.6	0.02
D_{sJ}^{*-} masses and widths	4.0	1.7	0.01
Fit with $D_{s3}^*(2860)^-$	0.3	2.5	0.05
$D^- - K_S^0$ K-matrix model	5.0	2.1	0.04
Total	7	6	0.2

pesudoexperiments [16], to be 5.3 standard deviations (σ) after accounting for systematic effects described later. If instead $J^P = 1^-$ is set for the $D^0 K_S^0$ resonance (denoted as T_{cs1}^{*0}), its width is determined to be around 5 GeV and the increase of the likelihood is only $2\Delta \ln \mathcal{L} = 12.2$. A fit, including two $D^0 K_S^0$ states (*i.e.* T_{cs0}^{*0} and T_{cs1}^{*0}) with $J^P = 0^+$ and 1^- respectively, has only a marginal improvement compared to the fit including only the T_{cs0}^{*0} state. Therefore, the contribution of any T_{cs1}^{*0} state is not significant.

Various systematic uncertainties are considered for the mass, width and FF measurements of the T_{cs0}^{*0} state, as summarized in Table 1. They are studied with alternative models, and largest deviations are taken as the systematic uncertainties. The uncertainty due to the B^- signal fraction f_s is studied by varying f_s within its uncertainty. The uncertainty due to the imperfect modeling of the background PDF in the amplitude fit is studied by using data samples with varied BDT selections to construct the distribution. The uncertainty due to the efficiency takes into account the contributions from residual mismodeling of the B^- kinematics, PID and hardware-level trigger responses by simulation, studied using alternative data-driven corrections. The uncertainty from the Blatt–Weisskopf radii are studied by varying from the default values of 4 (GeV/ c) $^{-1}$ to 3 or 5 (GeV/ c) $^{-1}$. The uncertainties due to known D_{sJ}^{*-} masses and widths are studied by floating these parameters in the amplitude fit with Gaussian constraints to known values. An additional $D_{s3}^*(2860)^-$ state is included in the amplitude fit to test the variation of the T_{cs0}^{*0} measurements. The D_{sJ}^{*-} model is also studied by using an alternative K-matrix model to describe the spin-1 $D^- K_S^0$ contributions. The total systematic uncertainties are determined by combining all contributions in quadrature, and are found to be smaller than the statistical uncertainties.

The mass, width and J^P of the T_{cs0}^{*0} state measured in the $D^0 K_S^0$ mass spectrum of the $B^- \rightarrow D^- D^0 K_S^0$ decay are consistent with those of the $T_{cs0}^*(2870)^0$ state observed in the $D^+ K^-$ mass spectrum of the $B^- \rightarrow D^- D^+ K^-$ decay [16], making them likely to be the same state. Under this hypothesis, alternative fits are performed constraining the masses and widths of $T_{cs0,1}^{*0}$ resonances to the known values of $T_{cs0}^*(2870)^0$ and $T_{cs1}^*(2900)^0$ states [42]. The fit fractions of the $T_{cs0}^*(2870)^0$ and $T_{cs1}^*(2900)^0$ states are measured to be $(2.6 \pm 0.9 \pm 0.5)\%$ and $(0.6 \pm 0.6 \pm 0.2)\%$ respectively, where the first uncertainties are statistical and the second systematic, and the systematic uncertainties include the

Table 2: Measurements of the relative rates of decays into the $D^0 K_S^0$ and $D^+ K^-$ final states for $T_{cs0}^*(2870)^0$ and $T_{cs1}^*(2900)^0$ states, $R_I(T_{cs0}^*(2870)^0)$ and $R_I(T_{cs1}^*(2900)^0)$, and the ratio of relative fit fractions $R_{\text{FF}}(D^0 K_S^0/D^+ K^-)$. The first, second and third uncertainties are statistical, systematic, and due to the external inputs of $B^- \rightarrow D^- D^+ K^-$ and $B^- \rightarrow D^- D^0 K_S^0$ branching fractions, respectively.

Observable	Result
$R_I(T_{cs0}^*(2870)^0)$	3.3 ± 1.1 ± 1.1 ± 1.1
$R_I(T_{cs1}^*(2900)^0)$	0.15 ± 0.15 ± 0.05 ± 0.05
$R_{\text{FF}}(K^0 K_S^0/D^+ K^-)$	0.044 ± 0.035 ± 0.020

sources listed in Table 1. The significance of the $T_{cs0}^*(2870)^0$ state is 6.4σ , while the $T_{cs1}^*(2900)^0$ state alone has only a marginal significance of 1.8σ , with effects of systematic uncertainties considered.

Isospin of genuine T_{cs}^{*0} states in the $D\bar{K}$ invariant-mass spectrum can be either $I = 0$ or 1. In either case, isospin symmetry requires the relative widths between the $T_{cs}^{*0} \rightarrow D^0 K_S^0$ and $T_{cs}^{*0} \rightarrow D^+ K^-$ decays to be $R_I(T_{cs}^{*0}) \equiv \Gamma(T_{cs}^{*0} \rightarrow D^0 \bar{K}^0)/\Gamma(T_{cs}^{*0} \rightarrow D^+ K^-) \approx 1$. In addition, the ratio between the fit fractions of the T_{cs1}^{*0} and T_{cs0}^{*0} states in the $B^- \rightarrow D^- D^0 K_S^0$ decay, $R_{\text{FF}}(D^0 K_S^0) \equiv \text{FF}(T_{cs1}^{*0} \rightarrow D^0 K_S^0)/\text{FF}(T_{cs0}^{*0} \rightarrow D^0 K_S^0)$ is expected to approximate that in the $B^- \rightarrow D^- D^+ K^-$ decay, $R_{\text{FF}}(D^+ K^-)$. Therefore the ratios $R_I(T_{cs}^{*0})$ and $R_{\text{FF}}(D^0 K_S^0/D^+ K^-) \equiv R_{\text{FF}}(D^0 K_S^0)/R_{\text{FF}}(D^+ K^-)$ provide precise tests of the isospin symmetry. The relative widths $R_I(T_{cs}^{*0})$ are calculated according to

$$R_I(T_{cs}^{*0}) = \frac{\mathcal{B}(B^- \rightarrow D^- D^0 \bar{K}^0) \text{FF}(T_{cs}^{*0} \rightarrow D^0 K_S^0)}{\mathcal{B}(B^- \rightarrow D^- D^+ K^-) \text{FF}(T_{cs}^{*0} \rightarrow D^+ K^-)}, \quad (1)$$

where $\text{FF}(T_{cs}^{*0} \rightarrow D^0 K_S^0)$ and $\text{FF}(T_{cs}^{*0} \rightarrow D^+ K^-)$ [16] are the fit fractions of the $T_{cs}^{*0} \rightarrow D^0 K_S^0$ and $T_{cs}^{*0} \rightarrow D^+ K^-$ components in the $B^- \rightarrow D^- D^0 K_S^0$ and $B^- \rightarrow D^- D^+ K^-$ decays, respectively, and $\mathcal{B}(B^- \rightarrow D^- D^0 \bar{K}^0)$ and $\mathcal{B}(B^- \rightarrow D^- D^+ K^-)$ are the respective branching fractions [42].

The quantities $R_I(T_{cs}^{*0})$ and $R_{\text{FF}}(D^0 K_S^0/D^+ K^-)$ are measured assuming the $T_{cs0,1}^{*0}$ states observed in the $B^- \rightarrow D^- D^+ K^-$ decay are also present in the $B^- \rightarrow D^- D^0 K_S^0$ decay. As shown in Table 2, the relative rate for the $T_{cs0}^*(2870)^0$ decays, $R_I(T_{cs0}^*(2870)^0)$, is consistent with the hypothesis of isospin invariance of a genuine state, although a fairly large isospin violation can not be excluded at the current precision. However, the relative rate for the $T_{cs1}^*(2900)^0$ decays $R_I(T_{cs1}^*(2900)^0)$ and the relative FF ratio $R_{\text{FF}}(D^0 K_S^0/D^+ K^-)$ are significantly smaller than unity, which indicates isospin violation between $T_{cs1}^*(2900)^0$ decays. The violation can be explained if the $T_{cs1}^*(2900)^0$ structure is caused by kinematic singularities of $B^- \rightarrow D^{(*)0} D_{sJ}^{(*)-} (\rightarrow D^- K^{(*)0})$ decays with final-state rescattering or if the $T_{cs1}^*(2900)^0$ structure as a genuine state does not have a definite isospin [38].

In conclusion, an amplitude analysis of the $B^- \rightarrow D^- D^0 K_S^0$ decay is performed, using pp collisions at center-of-mass energies 7, 8 and 13 TeV collected by the LHCb detector, corresponding to an integrated luminosity of 9 fb^{-1} . A spin-0 open-charm tetraquark

state, T_{cs0}^{*0} , is observed in the $D^0 K_S^0$ final state for the first time, with a significance of 5.3σ . The mass and width of this state, and the fit fraction in the $B^- \rightarrow D^- D^0 K_S^0$ decay are measured to be

$$\begin{aligned} M(T_{cs0}^{*0}) &= 2883 \pm 11 \pm 7 \text{ MeV}/c^2, \\ \Gamma(T_{cs0}^{*0}) &= 87_{-47}^{+22} \pm 6 \text{ MeV}, \\ \text{FF}(T_{cs0}^{*0} \rightarrow D^0 K_S^0) &= (2.6 \pm 1.2 \pm 0.2)\%, \end{aligned}$$

where the first uncertainties are statistical and the second systematic. The mass, width, spin-parity and flavor content are all consistent with those of the $T_{cs0}^*(2870)^0$ state observed in the $D^+ K^-$ invariant-mass spectrum of the $B^- \rightarrow D^- D^+ K^-$ decay [16]. No significant T_{cs}^{*0} states with $J^P = 1^-$ or charmonium-like tetraquarks are observed in the $B^- \rightarrow D^- D^0 K_S^0$ decay. With masses and widths constrained to known values, the $T_{cs0}^*(2870)^0$ state is observed with a significance of 6.4σ in the $B^- \rightarrow D^- D^0 K_S^0$ decay, while the $T_{cs1}^*(2900)^0$ state alone has a marginal significance of 1.8σ . Assuming $T_{cs0}^*(2870)^0$ and $T_{cs1}^*(2900)^0$ states to be genuine hadrons, a violation of isospin invariance between the $T_{cs1}^*(2900)^0 \rightarrow D^0 \bar{K}^0$ and the $T_{cs1}^*(2900)^0 \rightarrow D^+ K^-$ decay rates is indicated. On the other hand, the relative rate between the $T_{cs0}^*(2870)^0 \rightarrow D^0 \bar{K}^0$ and $T_{cs0}^*(2870)^0 \rightarrow D^+ K^-$ decays is consistent with an isospin invariance at current experimental precision. The study in this analysis helps to shed light on the nature of the $T_{cs0,1}^{*0}$ states, in particular on the resonance or kinematic singularity interpretations.

Acknowledgements

We express our gratitude to our colleagues in the CERN accelerator departments for the excellent performance of the LHC. We thank the technical and administrative staff at the LHCb institutes. We acknowledge support from CERN and from the national agencies: CAPES, CNPq, FAPERJ and FINEP (Brazil); MOST and NSFC (China); CNRS/IN2P3 (France); BMBF, DFG and MPG (Germany); INFN (Italy); NWO (Netherlands); MNiSW and NCN (Poland); MCID/IFA (Romania); MICIU and AEI (Spain); SNSF and SER (Switzerland); NASU (Ukraine); STFC (United Kingdom); DOE NP and NSF (USA). We acknowledge the computing resources that are provided by CERN, IN2P3 (France), KIT and DESY (Germany), INFN (Italy), SURF (Netherlands), PIC (Spain), GridPP (United Kingdom), CSCS (Switzerland), IFIN-HH (Romania), CBPF (Brazil), and Polish WLCG (Poland). We are indebted to the communities behind the multiple open-source software packages on which we depend. Individual groups or members have received support from ARC and ARDC (Australia); Key Research Program of Frontier Sciences of CAS, CAS PIFI, CAS CCEPP, Fundamental Research Funds for the Central Universities, and Sci. & Tech. Program of Guangzhou (China); Minciencias (Colombia); EPLANET, Marie Skłodowska-Curie Actions, ERC and NextGenerationEU (European Union); A*MIDEX, ANR, IPhU and Labex P2IO, and Région Auvergne-Rhône-Alpes (France); AvH Foundation (Germany); ICSC (Italy); Severo Ochoa and María de Maeztu Units of Excellence, GVA, XuntaGal, GENCAT, InTalent-Inditex and Prog. Atracción Talento CM (Spain); SRC (Sweden); the Leverhulme Trust, the Royal Society and UKRI (United Kingdom).

End Matter

1 Amplitude fit results using the nominal model

The nominal amplitude fit results are summarized in Table 3.

Table 3: Fit results of the parameters in the amplitude fit using the nominal amplitude model. The first uncertainty is statistical, and the second is systematic. The $\mathcal{R}e$, $\mathcal{I}m$, FF represent the real and imaginary part of the helicity couplings and the fit fraction respectively.

Decay channel	Parameter	Fit result
$B^- \rightarrow D_{s1}^*(2700)^- D^0$	$\mathcal{R}e$	1 (fixed)
	$\mathcal{I}m$	0 (fixed)
	FF	$0.271 \pm 0.029 \pm 0.018$
$B^- \rightarrow D_{s2}^*(2573)^- D^0$	$\mathcal{R}e$	$-0.043 \pm 0.019 \pm 0.042$
	$\mathcal{I}m$	$-0.109 \pm 0.019 \pm 0.040$
	FF	$0.0159 \pm 0.0047 \pm 0.0017$
$B^- \rightarrow D_{s1}^*(2860)^- D^0$	$\mathcal{R}e$	$-0.30 \pm 0.10 \pm 0.05$
	$\mathcal{I}m$	$0.45 \pm 0.10 \pm 0.18$
	FF	$0.060 \pm 0.015 \pm 0.009$
$B^- \rightarrow \text{NR (S-wave)} D^0$	$\mathcal{R}e$	$1.17 \pm 0.22 \pm 0.27$
	$\mathcal{I}m$	$-2.18 \pm 0.17 \pm 1.43$
	Slope	$0.476 \pm 0.033 \pm 0.015 \text{ (GeV}/c^2)^{-1}$
	FF	$0.449 \pm 0.030 \pm 0.038$
$B^- \rightarrow \text{NR (P-wave)} D^0$	$\mathcal{R}e$	$1.44 \pm 0.15 \pm 0.18$
	$\mathcal{I}m$	$0.21 \pm 0.17 \pm 0.08$
	FF	$0.271 \pm 0.034 \pm 0.021$
$B^- \rightarrow T_{cs0}^*(2870)^0 D^-$	$\mathcal{R}e$	$-0.12 \pm 0.04 \pm 0.04$
	$\mathcal{I}m$	$0.09 \pm 0.05 \pm 0.09$
	FF	$0.0259 \pm 0.0124 \pm 0.0017$
	Mass	$2883 \pm 11 \pm 7 \text{ MeV}/c^2$
	Width	$87 \pm_{47}^{22} \pm 6 \text{ MeV}$
Total fit fraction		1.093 ± 0.026

References

- [1] Y.-R. Liu *et al.*, *Pentaquark and tetraquark states*, *Prog. Part. Nucl. Phys.* **107** (2019) 237, [arXiv:1903.11976](#).
- [2] F.-K. Guo *et al.*, *Hadronic molecules*, *Rev. Mod. Phys.* **90** (2018) 015004, [arXiv:1705.00141](#).
- [3] Belle collaboration, S.-K. Choi *et al.*, *Observation of a narrow charmoniumlike state in exclusive $B^\pm \rightarrow K^\pm \pi^+ \pi^- J/\psi$ decays*, *Phys. Rev. Lett.* **91** (2003) 262001, [arXiv:hep-ex/0309032](#).
- [4] BESIII collaboration, M. Ablikim *et al.*, *Observation of a charged charmoniumlike structure in $e^+e^- \rightarrow \pi^+\pi^- J/\psi$ at $\sqrt{s} = 4.26$ GeV*, *Phys. Rev. Lett.* **110** (2013) 252001, [arXiv:1303.5949](#).
- [5] Belle collaboration, Z. Q. Liu *et al.*, *Study of $e^+e^- \rightarrow \pi^+\pi^- J/\psi$ and observation of a charged charmoniumlike state at Belle*, *Phys. Rev. Lett.* **110** (2013) 252002, [arXiv:1304.0121](#).
- [6] LHCb collaboration, R. Aaij *et al.*, *Observation of an exotic narrow doubly charmed tetraquark*, *Nature Physics* **18** (2022) 751, [arXiv:2109.01038](#).
- [7] LHCb collaboration, R. Aaij *et al.*, *Study of the doubly charmed tetraquark T_{cc}^+* , *Nature Communications* **13** (2022) 3351, [arXiv:2109.01056](#).
- [8] LHCb collaboration, R. Aaij *et al.*, *Observation of structure in the J/ψ -pair mass spectrum*, *Science Bulletin* **65** (2020) 1983, [arXiv:2006.16957](#).
- [9] ATLAS collaboration, G. Aad *et al.*, *Observation of an excess of dicharmonium events in the four-muon final state with the ATLAS detector*, *Phys. Rev. Lett.* **131** (2023) 151902, [arXiv:2304.08962](#).
- [10] CMS collaboration, A. Hayrapetyan *et al.*, *New structures in the $J/\psi J/\psi$ mass spectrum in proton-proton collisions at $\sqrt{s} = 13$ TeV*, *Phys. Rev. Lett.* **132** (2024) 111901, [arXiv:2306.07164](#).
- [11] LHCb collaboration, R. Aaij *et al.*, *Observation of $J/\psi p$ resonances consistent with pentaquark states in $\Lambda_b^0 \rightarrow J/\psi p K^-$ decays*, *Phys. Rev. Lett.* **115** (2015) 072001, [arXiv:1507.03414](#).
- [12] LHCb collaboration, R. Aaij *et al.*, *Observation of a narrow pentaquark state, $P_c(4312)^+$, and of two-peak structure of the $P_c(4450)^+$* , *Phys. Rev. Lett.* **122** (2019) 222001, [arXiv:1904.03947](#).
- [13] LHCb collaboration, R. Aaij *et al.*, *Evidence for a new structure in the $J/\psi p$ and $J/\psi \bar{p}$ systems in $B_s^0 \rightarrow J/\psi p \bar{p}$ decays*, *Phys. Rev. Lett.* **128** (2022) 062001, [arXiv:2108.04720](#).
- [14] LHCb collaboration, R. Aaij *et al.*, *Evidence of a $J/\psi \Lambda$ structure and observation of excited Ξ^- states in the $\Xi_b^- \rightarrow J/\psi \Lambda K^-$ decay*, *Science Bulletin* **66** (2021) 1278, [arXiv:2012.10380](#).


- [15] LHCb collaboration, R. Aaij *et al.*, *Observation of a $J/\psi\Lambda$ resonance consistent with a strange pentaquark candidate in $B^- \rightarrow J/\psi\Lambda\bar{p}$ decays*, *Phys. Rev. Lett.* **131** (2023) 031901, [arXiv:2210.10346](#).
- [16] LHCb collaboration, R. Aaij *et al.*, *Amplitude analysis of the $B^+ \rightarrow D^+D^-K^+$ decay*, *Phys. Rev.* **D102** (2020) 112003, [arXiv:2009.00026](#).
- [17] LHCb collaboration, R. Aaij *et al.*, *Model-independent study of structure in $B^+ \rightarrow D^+D^-K^+$ decays*, *Phys. Rev. Lett.* **125** (2020) 242001, [arXiv:2009.00025](#).
- [18] LHCb collaboration, R. Aaij *et al.*, *Observation of new charmonium or charmoniumlike states in $B^+ \rightarrow D^{*\pm}D^\mp K^+$ decays*, *Phys. Rev. Lett.* **133** (2024) 131902, [arXiv:2406.03156](#).
- [19] LHCb collaboration, R. Aaij *et al.*, *First observation of the $\Lambda_b^0 \rightarrow D^+D^-\Lambda$ decay*, *JHEP* **07** (2024) 140, [arXiv:2403.03586](#).
- [20] LHCb collaboration, R. Aaij *et al.*, *First observation of a doubly charged tetraquark candidate and its neutral partner*, *Phys. Rev. Lett.* **131** (2023) 041902, [arXiv:2212.02716](#).
- [21] LHCb collaboration, R. Aaij *et al.*, *Amplitude analysis of $B^0 \rightarrow \bar{D}^0D_s^+\pi^-$ and $B^+ \rightarrow D^-D_s^+\pi^+$ decays*, *Phys. Rev.* **D108** (2023) 012017, [arXiv:2212.02717](#).
- [22] M. Karliner and J. L. Rosner, *First exotic hadron with open heavy flavor: $cs\bar{u}\bar{d}$ tetraquark*, *Phys. Rev.* **D102** (2020) 094016, [arXiv:2008.05993](#).
- [23] X.-G. He, W. Wang, and R. Zhu, *Open-charm tetraquark X_c and open-bottom tetraquark X_b* , *Eur. Phys. J.* **C80** (2020) 1026, [arXiv:2008.07145](#).
- [24] T. Guo, J. Li, J. Zhao, and L. He, *Mass spectra and decays of open-heavy tetraquark states*, *Phys. Rev.* **D105** (2022) 054018, [arXiv:2108.06222](#).
- [25] U. Özdem and K. Azizi, *Magnetic moment of the $X_1(2900)$ state in the diquark-antidiquark picture*, *Eur. Phys. J.* **A58** (2022) 171, [arXiv:2202.11466](#).
- [26] Z.-G. Wang, *Analysis of the $X_0(2900)$ as the scalar tetraquark state via the QCD sum rules*, *Int. J. Mod. Phys.* **A35** (2020) 2050187, [arXiv:2008.07833](#).
- [27] S. S. Agaev, K. Azizi, and H. Sundu, *Vector resonance $X_1(2900)$ and its structure*, *Nucl. Phys.* **A1011** (2021) 122202, [arXiv:2103.06151](#).
- [28] G. Yang, J. Ping, and J. Segovia, *$sQ\bar{q}\bar{q}$ ($q = u, d$; $Q = c, b$) tetraquarks in the chiral quark model*, *Phys. Rev.* **D103** (2021) 074011, [arXiv:2101.04933](#).
- [29] G.-J. Wang *et al.*, *Mass spectrum and strong decays of tetraquark $\bar{c}sqq$ states*, *Eur. Phys. J.* **C81** (2021) 188, [arXiv:2010.09395](#).
- [30] M.-W. Hu, X.-Y. Lao, P. Ling, and Q. Wang, *$X_0(2900)$ and its heavy quark spin partners in molecular picture*, *Chin. Phys.* **C45** (2021) 021003, [arXiv:2008.06894](#).
- [31] M.-Z. Liu, J.-J. Xie, and L.-S. Geng, *$X_0(2866)$ as a $D^*\bar{K}^*$ molecular state*, *Phys. Rev.* **D102** (2020) 091502, [arXiv:2008.07389](#).

- [32] S.-Y. Kong, J.-T. Zhu, D. Song, and J. He, *Heavy-strange meson molecules and possible candidates $D_{s0}^*(2317)$, $D_{s1}(2460)$, and $X_0(2900)$* , *Phys. Rev.* **D104** (2021) 094012, [arXiv:2106.07272](#).
- [33] B. Wang and S.-L. Zhu, *How to understand the $X(2900)$?*, *Eur. Phys. J.* **C82** (2022) 419, [arXiv:2107.09275](#).
- [34] C.-J. Xiao, D.-Y. Chen, Y.-B. Dong, and G.-W. Meng, *Study of the decays of S -wave \bar{D}^*K^* hadronic molecules: the scalar $X_0(2900)$ and its spin partners $\tilde{X}_{J(J=1,2)}$* , *Phys. Rev.* **D103** (2021) 034004, [arXiv:2009.14538](#).
- [35] H.-X. Chen, W. Chen, R.-R. Dong, and N. Su, *$X_0(2900)$ and $X_1(2900)$: hadronic molecules or compact tetraquarks*, *Chin. Phys. Lett.* **37** (2020) 101201, [arXiv:2008.07516](#).
- [36] H.-X. Chen, *Covalent hadronic molecules induced by shared light quarks*, *Commun. Theor. Phys.* **74** (2022) 125201, [arXiv:2105.09193](#).
- [37] Y. Huang, J.-X. Lu, J.-J. Xie, and L.-S. Geng, *Strong decays of \bar{D}^*K^* molecules and the newly observed $X_{0,1}$ states*, *Eur. Phys. J.* **C80** (2020) 973, [arXiv:2008.07959](#).
- [38] T. J. Burns and E. S. Swanson, *Discriminating among interpretations for the $X(2900)$ states*, *Phys. Rev.* **D103** (2021) 014004, [arXiv:2009.05352](#).
- [39] H.-X. Chen *et al.*, *An updated review of the new hadron states*, *Rept. Prog. Phys.* **86** (2023) 026201, [arXiv:2204.02649](#).
- [40] LHCb collaboration, A. A. Alves Jr. *et al.*, *The LHCb detector at the LHC*, *JINST* **3** (2008) S08005.
- [41] LHCb collaboration, R. Aaij *et al.*, *LHCb detector performance*, *Int. J. Mod. Phys.* **A30** (2015) 1530022, [arXiv:1412.6352](#).
- [42] Particle Data Group, S. Navas *et al.*, *Review of particle physics*, *Phys. Rev.* **D110** (2024) 030001.
- [43] W. D. Hulsbergen, *Decay chain fitting with a Kalman filter*, *Nucl. Instrum. Meth.* **A552** (2005) 566, [arXiv:physics/0503191](#).
- [44] L. Breiman, J. H. Friedman, R. A. Olshen, and C. J. Stone, *Classification and regression trees*, Wadsworth international group, Belmont, California, USA, 1984.
- [45] Y. Freund and R. E. Schapire, *A decision-theoretic generalization of on-line learning and an application to boosting*, *J. Comput. Syst. Sci.* **55** (1997) 119.
- [46] H. Voss, A. Hoecker, J. Stelzer, and F. Tegenfeldt, *TMVA - Toolkit for Multivariate Data Analysis with ROOT*, *PoS ACAT* (2007) 040; A. Hoecker *et al.*, *TMVA 4 — Toolkit for Multivariate Data Analysis with ROOT. Users Guide.*, [arXiv:physics/0703039](#).
- [47] T. Sjöstrand, S. Mrenna, and P. Skands, *A brief introduction to PYTHIA 8.1*, *Comput. Phys. Commun.* **178** (2008) 852, [arXiv:0710.3820](#).

- [48] D. J. Lange, *The EvtGen particle decay simulation package*, [Nucl. Instrum. Meth. **A462** \(2001\) 152.](#)
- [49] Geant4 collaboration, J. Allison *et al.*, *Geant4 developments and applications*, [IEEE Trans. Nucl. Sci. **53** \(2006\) 270.](#)
- [50] D. Müller, M. Clemencic, G. Corti, and M. Gersabeck, *ReDecay: A novel approach to speed up the simulation at LHCb*, [Eur. Phys. J. **C78** \(2018\) 1009](#), [arXiv:1810.10362](#).
- [51] M. Jacob and G. C. Wick, *On the general theory of collisions for particles with spin*, [Annals Phys. **7** \(1959\) 404.](#)
- [52] J. Back *et al.*, *LAURA⁺⁺: A Dalitz plot fitter*, [Comput. Phys. Commun. **231** \(2018\) 198](#), [arXiv:1711.09854](#).
- [53] S. U. Chung *et al.*, *Partial wave analysis in K-matrix formalism*, [Annalen Phys. **4** \(1995\) 404.](#)

LHCb collaboration

R. Aaij³⁸, A.S.W. Abdelmotteleb⁵⁷, C. Abellan Beteta⁵¹, F. Abudinén⁵⁷,
T. Ackernley⁶¹, A. A. Adefisoye⁶⁹, B. Adeva⁴⁷, M. Adinolfi⁵⁵, P. Adlarson⁸²,
C. Agapopoulou¹⁴, C.A. Aidala⁸³, Z. Ajaltouni¹¹, S. Akar⁶⁶, K. Akiba³⁸,
P. Albicocco²⁸, J. Albrecht^{19,f}, F. Alessio⁴⁹, M. Alexander⁶⁰, Z. Aliouche⁶³,
P. Alvarez Cartelle⁵⁶, R. Amalric¹⁶, S. Amato³, J.L. Amey⁵⁵, Y. Amhis¹⁴,
L. An⁶, L. Anderlini²⁷, M. Andersson⁵¹, A. Andreianov⁴⁴, P. Andreola⁵¹,
M. Andreotti²⁶, D. Andreou⁶⁹, A. Anelli^{31,o}, D. Ao⁷, F. Archilli^{37,u},
M. Argenton²⁶, S. Arguedas Cuendis^{9,49}, A. Artamonov⁴⁴, M. Artuso⁶⁹,
E. Aslanides¹³, R. Ataíde Da Silva⁵⁰, M. Atzeni⁶⁵, B. Audurier¹², D. Bacher⁶⁴,
I. Bachiller Perea¹⁰, S. Bachmann²², M. Bachmayer⁵⁰, J.J. Back⁵⁷,
P. Baladron Rodriguez⁴⁷, V. Balagura¹⁵, A. Balboni²⁶, W. Baldini²⁶, L. Balzani¹⁹,
H. Bao⁷, J. Baptista de Souza Leite⁶¹, C. Barbero Pretel^{47,12}, M. Barbetti²⁷,
R. Barbosa⁷⁰, R.J. Barlow⁶³, M. Barnyakov²⁵, S. Barsuk¹⁴, W. Barter⁵⁹,
M. Bartolini⁵⁶, J. Bartz⁶⁹, J.M. Basels¹⁷, S. Bashir⁴⁰, G. Bassi^{35,r}, B. Batsukh⁵,
P. B. Battista¹⁴, A. Bay⁵⁰, A. Beck⁵⁷, M. Becker¹⁹, F. Bedeschi³⁵, I.B. Bediaga²,
N. A. Behling¹⁹, S. Belin⁴⁷, K. Belous⁴⁴, I. Belov²⁹, I. Belyaev³⁶, G. Benane¹³,
G. Bencivenni²⁸, E. Ben-Haim¹⁶, A. Berezhnoy⁴⁴, R. Bernet⁵¹, S. Bernet Andres⁴⁵,
A. Bertolin³³, C. Betancourt⁵¹, F. Betti⁵⁹, J. Bex⁵⁶, Ia. Bezshyiko⁵¹, J. Bhom⁴¹,
M.S. Bieker¹⁹, N.V. Biesuz²⁶, P. Billoir¹⁶, A. Biolchini³⁸, M. Birch⁶²,
F.C.R. Bishop¹⁰, A. Bitadze⁶³, A. Bizzeti¹⁰, T. Blake⁵⁷, F. Blanc⁵⁰, J.E. Blank¹⁹,
S. Blusk⁶⁹, V. Bocharnikov⁴⁴, J.A. Boelhaue¹⁹, O. Boente Garcia¹⁵,
T. Boettcher⁶⁶, A. Bohare⁵⁹, A. Boldyrev⁴⁴, C.S. Bolognani⁷⁹, R. Bolzonella^{26,l},
R. B. Bonacci¹, N. Bondar⁴⁴, A. Bordelius⁴⁹, F. Borgato^{33,p}, S. Borghi⁶³,
M. Borsato^{31,o}, J.T. Borsuk⁴¹, S.A. Bouchiba⁵⁰, M. Bovill⁶⁴, T.J.V. Bowcock⁶¹,
A. Boyer⁴⁹, C. Bozzi²⁶, A. Brea Rodriguez⁵⁰, N. Breer¹⁹, J. Brodzicka⁴¹,
A. Brossa Gonzalo^{47,†}, J. Brown⁶¹, D. Brundu³², E. Buchanan⁵⁹, A. Buonauro⁵¹,
L. Buonincontri^{33,p}, A.T. Burke⁶³, C. Burr⁴⁹, J.S. Butter⁵⁶, J. Buytaert⁴⁹,
W. Byczynski⁴⁹, S. Cadeddu³², H. Cai⁷⁴, A. C. Caillet¹⁶, R. Calabrese^{26,l},
S. Calderon Ramirez⁹, L. Calefice⁴⁶, S. Cali²⁸, M. Calvi^{31,o}, M. Calvo Gomez⁴⁵,
P. Camargo Magalhaes^{2,y}, J. I. Cambon Bouzas⁴⁷, P. Campana²⁸,
D.H. Campora Perez⁷⁹, A.F. Campoverde Quezada⁷, S. Capelli³¹, L. Capriotti²⁶,
R. Caravaca-Mora⁹, A. Carbone^{25,j}, L. Carcedo Salgado⁴⁷, R. Cardinale^{29,m},
A. Cardini³², P. Carniti^{31,o}, L. Carus²², A. Casais Vidal⁶⁵, R. Caspary²²,
G. Casse⁶¹, M. Cattaneo⁴⁹, G. Cavallero^{26,49}, V. Cavallini^{26,l}, S. Celani²²,
D. Cervenkov⁶⁴, S. Cesare^{30,n}, A.J. Chadwick⁶¹, I. Chahrouh⁸³, M. Charles¹⁶,
Ph. Charpentier⁴⁹, E. Chatzianagnostou³⁸, M. Chefdeville¹⁰, C. Chen¹³, S. Chen⁵,
Z. Chen⁷, A. Chernov⁴¹, S. Chernyshenko⁵³, X. Chiotopoulos⁷⁹, V. Chobanova⁸¹,
S. Cholak⁵⁰, M. Chruszacz⁴¹, A. Chubykin⁴⁴, V. Chulikov²⁸, P. Ciambone²⁸,
X. Cid Vidal⁴⁷, G. Ciezarek⁴⁹, P. Cifra⁴⁹, P.E.L. Clarke⁵⁹, M. Clemencic⁴⁹,
H.V. Cliff⁵⁶, J. Closier⁴⁹, C. Cocha Toapaxi²², V. Coco⁴⁹, J. Cogan¹³,
E. Cogneras¹¹, L. Cojocariu⁴³, S. Collaviti⁵⁰, P. Collins⁴⁹, T. Colombo⁴⁹,
M. Colonna¹⁹, A. Comerma-Montells⁴⁶, L. Congedo²⁴, A. Contu³², N. Cooke⁶⁰,
I. Corredoira⁴⁷, A. Correia¹⁶, G. Corti⁴⁹, J.J. Cottee Meldrum⁵⁵, B. Couturier⁴⁹,
D.C. Craik⁵¹, M. Cruz Torres^{2,g}, E. Curras Rivera⁵⁰, R. Currie⁵⁹, C.L. Da Silva⁶⁸,
S. Dadabaev⁴⁴, L. Dai⁷¹, X. Dai⁶, E. Dall’Occo⁴⁹, J. Dalseno⁴⁷,
C. D’Ambrosio⁴⁹, J. Daniel¹¹, A. Danilina⁴⁴, P. d’Argent²⁴, G. Darze³, A.
Davidson⁵⁷, J.E. Davies⁶³, A. Davis⁶³, O. De Aguiar Francisco⁶³, C. De Angelis^{32,k},
F. De Benedetti⁴⁹, J. de Boer³⁸, K. De Bruyn⁷⁸, S. De Capua⁶³, M. De Cian²²,

U. De Freitas Carneiro Da Graca^{2,a} , E. De Lucia²⁸ , J.M. De Miranda² , L. De Paula³ ,
 M. De Serio^{24,h} , P. De Simone²⁸ , F. De Vellis¹⁹ , J.A. de Vries⁷⁹ , F. Debernardis²⁴ ,
 D. Decamp¹⁰ , V. Dedu¹³ , S. Dekkers¹ , L. Del Buono¹⁶ , B. Delaney⁶⁵ ,
 H.-P. Dembinski¹⁹ , J. Deng⁸ , V. Denysenko⁵¹ , O. Deschamps¹¹ , F. Dettori^{32,k} ,
 B. Dey⁷⁷ , P. Di Nezza²⁸ , I. Diachkov⁴⁴ , S. Didenko⁴⁴ , S. Ding⁶⁹ , L. Dittmann²² ,
 V. Dobishuk⁵³ , A. D. Docheva⁶⁰ , C. Dong^{4,b} , A.M. Donohoe²³ , F. Dordei³² ,
 A.C. dos Reis² , A. D. Dowling⁶⁹ , W. Duan⁷² , P. Duda⁸⁰ , M.W. Dudek⁴¹ ,
 L. Dufour⁴⁹ , V. Duk³⁴ , P. Durante⁴⁹ , M. M. Duras⁸⁰ , J.M. Durham⁶⁸ , O. D.
 Durmus⁷⁷ , A. Dziurda⁴¹ , A. Dzyuba⁴⁴ , S. Easo⁵⁸ , E. Eckstein¹⁸ , U. Egede¹ ,
 A. Egorychev⁴⁴ , V. Egorychev⁴⁴ , S. Eisenhardt⁵⁹ , E. Ejopu⁶³ , L. Eklund⁸² ,
 M. Elashri⁶⁶ , J. Ellbracht¹⁹ , S. Ely⁶² , A. Ene⁴³ , J. Eschle⁶⁹ , S. Esen²² ,
 T. Evans⁶³ , F. Fabiano^{32,k} , L.N. Falcao² , Y. Fan⁷ , B. Fang⁷ , L. Fantini^{34,q,49} ,
 M. Faria⁵⁰ , K. Farmer⁵⁹ , D. Fazzini^{31,o} , L. Felkowski⁸⁰ , M. Feng^{5,7} , M. Feo¹⁹ ,
 A. Fernandez Casani⁴⁸ , M. Fernandez Gomez⁴⁷ , A.D. Fernez⁶⁷ , F. Ferrari²⁵ ,
 F. Ferreira Rodrigues³ , M. Ferrillo⁵¹ , M. Ferro-Luzzi⁴⁹ , S. Filippov⁴⁴ , R.A. Fini²⁴ ,
 M. Fiorini^{26,l} , M. Firlej⁴⁰ , K.L. Fischer⁶⁴ , D.S. Fitzgerald⁸³ , C. Fitzpatrick⁶³ ,
 T. Fiutowski⁴⁰ , F. Fleuret¹⁵ , M. Fontana²⁵ , L. F. Foreman⁶³ , R. Forty⁴⁹ ,
 D. Foulds-Holt⁵⁶ , V. Franco Lima³ , M. Franco Sevilla⁶⁷ , M. Frank⁴⁹ ,
 E. Franzoso^{26,l} , G. Frau⁶³ , C. Frei⁴⁹ , D.A. Friday⁶³ , J. Fu⁷ , Q. Führung^{19,f,56} ,
 Y. Fujii¹ , T. Fulghesu¹⁶ , E. Gabriel³⁸ , G. Galati²⁴ , M.D. Galati³⁸ ,
 A. Gallas Torreira⁴⁷ , D. Galli^{25,j} , S. Gambetta⁵⁹ , M. Gandelman³ , P. Gandini³⁰ , B.
 Ganie⁶³ , H. Gao⁷ , R. Gao⁶⁴ , T.Q. Gao⁵⁶ , Y. Gao⁸ , Y. Gao⁶ , Y. Gao⁸,
 L.M. Garcia Martin⁵⁰ , P. Garcia Moreno⁴⁶ , J. García Pardiñas⁴⁹ , P. Gardner⁶⁷ , K. G.
 Garg⁸ , L. Garrido⁴⁶ , C. Gaspar⁴⁹ , R.E. Geertsema³⁸ , L.L. Gerken¹⁹ ,
 E. Gersabeck⁶³ , M. Gersabeck²⁰ , T. Gershon⁵⁷ , S. Ghizzo^{29,m},
 Z. Ghorbanimoghaddam⁵⁵, L. Giambastiani^{33,p} , F. I. Giasemis^{16,e} , V. Gibson⁵⁶ ,
 H.K. Giemza⁴² , A.L. Gilman⁶⁴ , M. Giovannetti²⁸ , A. Gioventù⁴⁶ , L. Girardey⁶³ ,
 P. Gironella Gironell⁴⁶ , C. Giugliano^{26,l} , M.A. Giza⁴¹ , E.L. Gkoukousis⁶² ,
 F.C. Glaser^{14,22} , V.V. Gligorov^{16,49} , C. Göbel⁷⁰ , E. Golobardes⁴⁵ , D. Golubkov⁴⁴ ,
 A. Golutvin^{62,44,49} , S. Gomez Fernandez⁴⁶ , W. Gomulka⁴⁰, F. Goncalves Abrantes⁶⁴ ,
 M. Goncerz⁴¹ , G. Gong^{4,b} , J. A. Gooding¹⁹ , I.V. Gorelov⁴⁴ , C. Gotti³¹ ,
 J.P. Grabowski¹⁸ , L.A. Granado Cardoso⁴⁹ , E. Graugés⁴⁶ , E. Graverini^{50,s} ,
 L. Grazette⁵⁷ , G. Graziani , A. T. Grecu⁴³ , L.M. Greeven³⁸ , N.A. Grieser⁶⁶ ,
 L. Grillo⁶⁰ , S. Gromov⁴⁴ , C. Gu¹⁵ , M. Guarise²⁶ , L. Guerry¹¹ , M. Guittiere¹⁴ ,
 V. Guliaeva⁴⁴ , P. A. Günther²² , A.-K. Guseinov⁵⁰ , E. Gushchin⁴⁴ , Y. Guz^{6,49,44} ,
 T. Gys⁴⁹ , K. Habermann¹⁸ , T. Hadavizadeh¹ , C. Hadjivasiliou⁶⁷ , G. Haefeli⁵⁰ ,
 C. Haen⁴⁹ , M. Hajheidari⁴⁹, G. Hallett⁵⁷ , M.M. Halvorsen⁴⁹ , P.M. Hamilton⁶⁷ ,
 J. Hammerich⁶¹ , Q. Han⁸ , X. Han^{22,49} , S. Hansmann-Menzemer²² , L. Hao⁷ ,
 N. Harnew⁶⁴ , T. H. Harris¹ , M. Hartmann¹⁴ , S. Hashmi⁴⁰ , J. He^{7,c} ,
 F. Hemmer⁴⁹ , C. Henderson⁶⁶ , R.D.L. Henderson^{1,57} , A.M. Hennequin⁴⁹ ,
 K. Hennessy⁶¹ , L. Henry⁵⁰ , J. Herd⁶² , P. Herrero Gascon²² , J. Heuel¹⁷ ,
 A. Hicheur³ , G. Hijano Mendizabal⁵¹, J. Horswill⁶³ , R. Hou⁸ , Y. Hou¹¹ ,
 N. Howarth⁶¹ , J. Hu⁷² , W. Hu⁶ , X. Hu^{4,b} , W. Huang⁷ , W. Hulsbergen³⁸ ,
 R.J. Hunter⁵⁷ , M. Hushchyn⁴⁴ , D. Hutchcroft⁶¹ , M. Idzik⁴⁰ , D. Ilin⁴⁴ , P. Ilten⁶⁶ ,
 A. Inglessi⁴⁴ , A. Iniukhin⁴⁴ , A. Ishteev⁴⁴ , K. Ivshin⁴⁴ , R. Jacobsson⁴⁹ , H. Jage¹⁷ ,
 S.J. Jaimes Elles^{75,49,48} , S. Jakobsen⁴⁹ , E. Jans³⁸ , B.K. Jashal⁴⁸ , A. Jawahery^{67,49} ,
 V. Jevtic^{19,f} , E. Jiang⁶⁷ , X. Jiang^{5,7} , Y. Jiang⁷ , Y. J. Jiang⁶ , M. John⁶⁴ , A.
 John Rubesh Rajan²³ , D. Johnson⁵⁴ , C.R. Jones⁵⁶ , T.P. Jones⁵⁷ , S. Joshi⁴² ,
 B. Jost⁴⁹ , J. Juan Castella⁵⁶ , N. Jurik⁴⁹ , I. Juszczak⁴¹ , D. Kaminaris⁵⁰ ,
 S. Kandybei⁵² , M. Kane⁵⁹ , Y. Kang^{4,b} , C. Kar¹¹ , M. Karacson⁴⁹ ,

- ²⁰ *Physikalisches Institut, Albert-Ludwigs-Universität Freiburg, Freiburg, Germany*
- ²¹ *Max-Planck-Institut für Kernphysik (MPIK), Heidelberg, Germany*
- ²² *Physikalisches Institut, Ruprecht-Karls-Universität Heidelberg, Heidelberg, Germany*
- ²³ *School of Physics, University College Dublin, Dublin, Ireland*
- ²⁴ *INFN Sezione di Bari, Bari, Italy*
- ²⁵ *INFN Sezione di Bologna, Bologna, Italy*
- ²⁶ *INFN Sezione di Ferrara, Ferrara, Italy*
- ²⁷ *INFN Sezione di Firenze, Firenze, Italy*
- ²⁸ *INFN Laboratori Nazionali di Frascati, Frascati, Italy*
- ²⁹ *INFN Sezione di Genova, Genova, Italy*
- ³⁰ *INFN Sezione di Milano, Milano, Italy*
- ³¹ *INFN Sezione di Milano-Bicocca, Milano, Italy*
- ³² *INFN Sezione di Cagliari, Monserrato, Italy*
- ³³ *INFN Sezione di Padova, Padova, Italy*
- ³⁴ *INFN Sezione di Perugia, Perugia, Italy*
- ³⁵ *INFN Sezione di Pisa, Pisa, Italy*
- ³⁶ *INFN Sezione di Roma La Sapienza, Roma, Italy*
- ³⁷ *INFN Sezione di Roma Tor Vergata, Roma, Italy*
- ³⁸ *Nikhef National Institute for Subatomic Physics, Amsterdam, Netherlands*
- ³⁹ *Nikhef National Institute for Subatomic Physics and VU University Amsterdam, Amsterdam, Netherlands*
- ⁴⁰ *AGH - University of Krakow, Faculty of Physics and Applied Computer Science, Kraków, Poland*
- ⁴¹ *Henryk Niewodniczanski Institute of Nuclear Physics Polish Academy of Sciences, Kraków, Poland*
- ⁴² *National Center for Nuclear Research (NCBJ), Warsaw, Poland*
- ⁴³ *Horia Hulubei National Institute of Physics and Nuclear Engineering, Bucharest-Magurele, Romania*
- ⁴⁴ *Affiliated with an institute covered by a cooperation agreement with CERN*
- ⁴⁵ *DS4DS, La Salle, Universitat Ramon Llull, Barcelona, Spain*
- ⁴⁶ *ICCUB, Universitat de Barcelona, Barcelona, Spain*
- ⁴⁷ *Instituto Galego de Física de Altas Enerxías (IGFAE), Universidade de Santiago de Compostela, Santiago de Compostela, Spain*
- ⁴⁸ *Instituto de Física Corpuscular, Centro Mixto Universidad de Valencia - CSIC, Valencia, Spain*
- ⁴⁹ *European Organization for Nuclear Research (CERN), Geneva, Switzerland*
- ⁵⁰ *Institute of Physics, Ecole Polytechnique Fédérale de Lausanne (EPFL), Lausanne, Switzerland*
- ⁵¹ *Physik-Institut, Universität Zürich, Zürich, Switzerland*
- ⁵² *NSC Kharkiv Institute of Physics and Technology (NSC KIPT), Kharkiv, Ukraine*
- ⁵³ *Institute for Nuclear Research of the National Academy of Sciences (KINR), Kyiv, Ukraine*
- ⁵⁴ *School of Physics and Astronomy, University of Birmingham, Birmingham, United Kingdom*
- ⁵⁵ *H.H. Wills Physics Laboratory, University of Bristol, Bristol, United Kingdom*
- ⁵⁶ *Cavendish Laboratory, University of Cambridge, Cambridge, United Kingdom*
- ⁵⁷ *Department of Physics, University of Warwick, Coventry, United Kingdom*
- ⁵⁸ *STFC Rutherford Appleton Laboratory, Didcot, United Kingdom*
- ⁵⁹ *School of Physics and Astronomy, University of Edinburgh, Edinburgh, United Kingdom*
- ⁶⁰ *School of Physics and Astronomy, University of Glasgow, Glasgow, United Kingdom*
- ⁶¹ *Oliver Lodge Laboratory, University of Liverpool, Liverpool, United Kingdom*
- ⁶² *Imperial College London, London, United Kingdom*
- ⁶³ *Department of Physics and Astronomy, University of Manchester, Manchester, United Kingdom*
- ⁶⁴ *Department of Physics, University of Oxford, Oxford, United Kingdom*
- ⁶⁵ *Massachusetts Institute of Technology, Cambridge, MA, United States*
- ⁶⁶ *University of Cincinnati, Cincinnati, OH, United States*
- ⁶⁷ *University of Maryland, College Park, MD, United States*
- ⁶⁸ *Los Alamos National Laboratory (LANL), Los Alamos, NM, United States*
- ⁶⁹ *Syracuse University, Syracuse, NY, United States*
- ⁷⁰ *Pontifícia Universidade Católica do Rio de Janeiro (PUC-Rio), Rio de Janeiro, Brazil, associated to ³*
- ⁷¹ *School of Physics and Electronics, Hunan University, Changsha City, China, associated to ⁸*
- ⁷² *Guangdong Provincial Key Laboratory of Nuclear Science, Guangdong-Hong Kong Joint Laboratory of Quantum Matter, Institute of Quantum Matter, South China Normal University, Guangzhou, China,*

associated to ⁴

⁷³ Lanzhou University, Lanzhou, China, associated to ⁵

⁷⁴ School of Physics and Technology, Wuhan University, Wuhan, China, associated to ⁴

⁷⁵ Departamento de Física , Universidad Nacional de Colombia, Bogota, Colombia, associated to ¹⁶

⁷⁶ Ruhr Universitaet Bochum, Fakultaet f. Physik und Astronomie, Bochum, Germany, associated to ¹⁹

⁷⁷ Eotvos Lorand University, Budapest, Hungary, associated to ⁴⁹

⁷⁸ Van Swinderen Institute, University of Groningen, Groningen, Netherlands, associated to ³⁸

⁷⁹ Universiteit Maastricht, Maastricht, Netherlands, associated to ³⁸

⁸⁰ Tadeusz Kosciuszko Cracow University of Technology, Cracow, Poland, associated to ⁴¹

⁸¹ Universidad de Coruña, A Coruña, Spain, associated to ⁴⁵

⁸² Department of Physics and Astronomy, Uppsala University, Uppsala, Sweden, associated to ⁶⁰

⁸³ University of Michigan, Ann Arbor, MI, United States, associated to ⁶⁹

^a Centro Federal de Educação Tecnológica Celso Suckow da Fonseca, Rio De Janeiro, Brazil

^b Center for High Energy Physics, Tsinghua University, Beijing, China

^c Hangzhou Institute for Advanced Study, UCAS, Hangzhou, China

^d School of Physics and Electronics, Henan University , Kaifeng, China

^e LIP6, Sorbonne Université, Paris, France

^f Lamarr Institute for Machine Learning and Artificial Intelligence, Dortmund, Germany

^g Universidad Nacional Autónoma de Honduras, Tegucigalpa, Honduras

^h Università di Bari, Bari, Italy

ⁱ Università di Bergamo, Bergamo, Italy

^j Università di Bologna, Bologna, Italy

^k Università di Cagliari, Cagliari, Italy

^l Università di Ferrara, Ferrara, Italy

^m Università di Genova, Genova, Italy

ⁿ Università degli Studi di Milano, Milano, Italy

^o Università degli Studi di Milano-Bicocca, Milano, Italy

^p Università di Padova, Padova, Italy

^q Università di Perugia, Perugia, Italy

^r Scuola Normale Superiore, Pisa, Italy

^s Università di Pisa, Pisa, Italy

^t Università della Basilicata, Potenza, Italy

^u Università di Roma Tor Vergata, Roma, Italy

^v Università di Siena, Siena, Italy

^w Università di Urbino, Urbino, Italy

^x Universidad de Alcalá, Alcalá de Henares , Spain

^y Facultad de Ciencias Físicas, Madrid, Spain

^z Department of Physics/Division of Particle Physics, Lund, Sweden

† Deceased